Geomorphology 118 (2010) 65–79

Contents lists available at ScienceDirect

Geomorphology

journal homepage: www.elsevier.com/locate/geomorph

Avulsion in action: Reconstruction and modelling sedimentation pace and upstream flood water levels following a Medieval tidal-river diversion catastrophe (Biesbosch, The Netherlands, 1421–1750 AD)

Maarten G. Kleinhans [a,*], Henk J.T. Weerts [b], Kim M. Cohen [a,1]

[a] Faculty of Geosciences, Department of Physical Geography, Utrecht University, PO Box 80115, 3508 TC Utrecht, The Netherlands
[b] Cultural Heritage Agency, PO Box 1600, 3800 BP Amersfoort, The Netherlands

ARTICLE INFO

Article history:
Received 23 June 2009
Received in revised form 3 December 2009
Accepted 9 December 2009
Available online 24 December 2009

Keywords:
Storm surge
River floods
Avulsion
Tidal flood basin
Delta
Crevasse splay

ABSTRACT

Deltaic land inundated by storm surges may reform by sedimentation from natural or human-induced river diversions. This is a well-known trigger mechanism for creation of new channels in coastal plains and deltas, which may develop into main channels and lead to abandonment of older (avulsion), particularly in the downstream parts of deltas that host tidal rivers. These new channels develop as part of deltaic splay complexes that heal initial diversion scars and fill up flooded basins at a certain pace.

We study a case with excellent historical and geological data of a diversion of the river Rhine following catastrophic inundations (1421–1424 AD) into medieval reclaimed land. Numerical modelling of deltaic splay and channel development is combined with reconstructions from historical maps and geological data. This yields detailed insight in pacing of splay sedimentation and changing hydrodynamics in the channel upstream of the diversion in the two centuries following the inundation.

The equivalent of the full sand budget of the river Rhine was effectively trapped in the developing splay. The tidal-avulsion splay evolution on aspects is similar to that of fluvial crevassing into flood basins documented for settings lacking 'downstream' tidal control. The typical small-scale delta-lobe avulsion cycles: mouth bar formation, backward sedimentation, upstream avulsion, channel progradation and mouth bar formation are reproduced in the splay-modelling. The pacing of splay development, however, is relatively fast due to the presence of tides and the water depth in the receiving basin. The diversion had a strong upstream impact, in particular on water levels in the feeding river channel at stages of peak flow. For two centuries levels were significantly raised, because bifurcation-imposed reduced transport capacity and associated sedimentation at the diversion site increased hydraulic roughness and hampered flow.

These findings have implications regarding flood mitigation for presently-planned lower-delta engineered diversions. Furthermore, they elucidate the differences between upstream fluvial avulsion and downstream tidal-river avulsion that are important to recognise if we want to understand how deltaic distributary-networks are maintained.

© 2009 Elsevier B.V. All rights reserved.

1. Introduction

River diversion leads to formation of inland deltas, crevasse splays and new river branches (bifurcation and avulsion). These affect sedimentary architecture and geomorphology of lowlands (Smith et al., 1989; Slingerland and Smith, 1998; Stouthamer and Berendsen, 2000) which has relevance for modern and ancient reservoir characterisation, fluvial morphodynamics and sedimentology, nature restoration and water management.

We study a river diversion and the formation of a deltaic splay (60 km^2, up to 4 m thick) within the larger lagoon-deltaic plain of the Holocene Rhine-Meuse delta (about 1000 km^2, 10–20 m thick). As such it is an element of the high-stand systems tract constituting the upper strata of the modern deltaic wedge. The diversion occurred inland in the former lagoon, in relatively protected position behind the 'Holland' coastal barrier system (wave-dominated coastline) which was penetrated by a series of storm surge-enlarged estuaries (e.g. Berendsen (1998); Fig. 1). Centuries after the area had been reclaimed by humans, the diversion formed catastrophically when a levee was breached (1421–1424 AD) and after this event a deltaic splay developed naturally for two centuries (see details below).

The splay filled a freshwater-tidal flood basin which makes this case of river diversion critically different from typically studied river avulsions higher up on the delta-plain, where tides do not play a role.

* Corresponding author. Tel.: +31 30 2532405; fax: +31 30 2531145.
E-mail addresses: m.kleinhans@geo.uu.nl (M.G. Kleinhans), h.weerts@cultureelerfgoed.nl (H.J.T. Weerts), k.cohen@geo.uu.nl (K.M. Cohen).
URL: http://www.geog.uu.nl/fg/mkleinhans (M.G. Kleinhans).
[1] Also at Deltares Geological Survey of the Netherlands.

0169-555X/$ – see front matter © 2009 Elsevier B.V. All rights reserved.
doi:10.1016/j.geomorph.2009.12.009

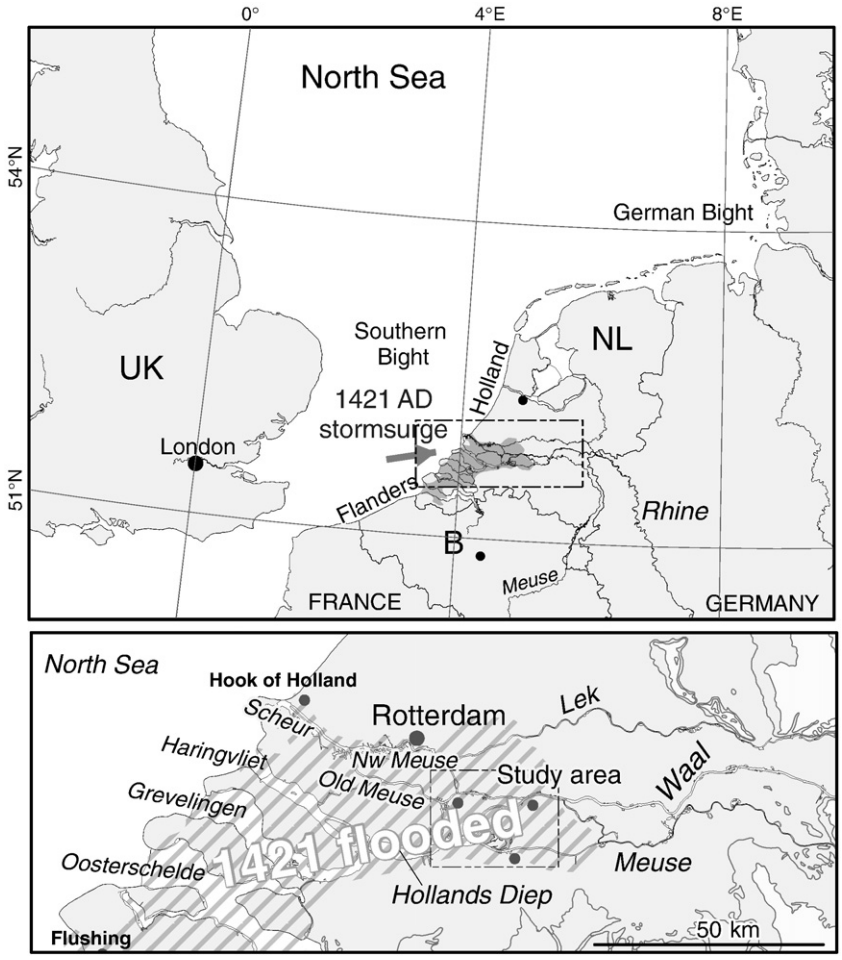

Fig. 1. Extent of 1421 storm surge and location of study area (Biesbosch basin deltaic splay). NL = Netherlands, B = Belgium, UK = United Kingdom.

The inland tidal-river diversion case is equally different from channel diversion at the very mouth of rivers that progradate into open water forming fluvial-dominated coastlines.

We regard a diversion a successful avulsion when the newly created tidal river draws over 50% of the discharge of the upstream channel (in bankfull conditions), implying sustained loss of discharge and partial infilling of the preexisting channel downstream of the diversion, if not total abandonment. The partial infilling case is called partial avulsion and the total abandonment full avulsion (cf. Stouthamer and Berendsen, 2000). The success of an avulsion, however, is to be determined following initial stages of avulsion development which besides morphodynamic adaptations in preexisting channels involves the build up of the diversion-splay (healing the breach and filling the flood basin) and the simultaneous, counteractive formation of dissective channels through it (routing diverted discharge), in complex interaction, as studied in this paper.

Studies of river diversions on coastal plains and their sedimentary products so far could not resolve the pace of splay sedimentation in relation to transport capacity of the original channel and the diversion, nor associated hydrodynamic changes. Geological data document the end result (deltaic body) but rarely bear sufficient detail to resolve the evolution. Morphodynamic modelling in principle delivers time-constrained evolution but realistic simulation requires detailed initial and boundary conditions. These conditions are typically unknown which makes key elements of model performance difficult to verify. Yet deeper understanding and predictability are essential for interpretation of modern and ancient sedimentary successions and to plan future land recovery and mitigate inundation risks from the river and the sea.

The setting of our study is a flood basin in the western Rhine delta, The Netherlands (Figs. 1 and 2), that had been reclaimed in Medieval times and was inundated by two storm surges from the North Sea and two floods of the river Rhine between 1421 and 1424 AD, commonly known as the St. Elisabeth flood. The inundation was catastrophic due to poor dike maintenance that led to loss of human life and major land loss. An extensive deltaic splay of limited thickness and a fan angle of about 90° developed in the inland tidal basin while several minor and one major tidal-river channels of up to 10 m deep at the apex shifted over the fan. In about two centuries half the inundated area had been filled up by the shallow splay (Fig. 3). Preservation of several historical maps and accessibility for geological study as well as familiarity with the context of the Rhine delta provide an opportunity to study this avulsion in detail and apply well-constrained morphodynamic modelling.

The objectives are to: i) understand what factors determine the initiation of a river diversion; ii) quantify the pacing and morphology of sedimentation generically; and iii) assess quantitatively the effect of sedimentation on upstream flood water levels.

Complementary sources of information are combined. First, historical studies, sources and maps are presented, after which the detailed clues on the nature of the events during and after the St. Elisabeth flood are inferred. Second, we elaborate on how we used geological data from core descriptions to quantify the sand budget and construct geological coring transects to characterise the deposits and provide clues on the formative mechanisms. Third, we describe a state-of-the-art two-dimensional flow and morphodynamical model that we used to model flow and general evolution of the deltaic splay over a period of two centuries following flooding. Various pieces of information remain

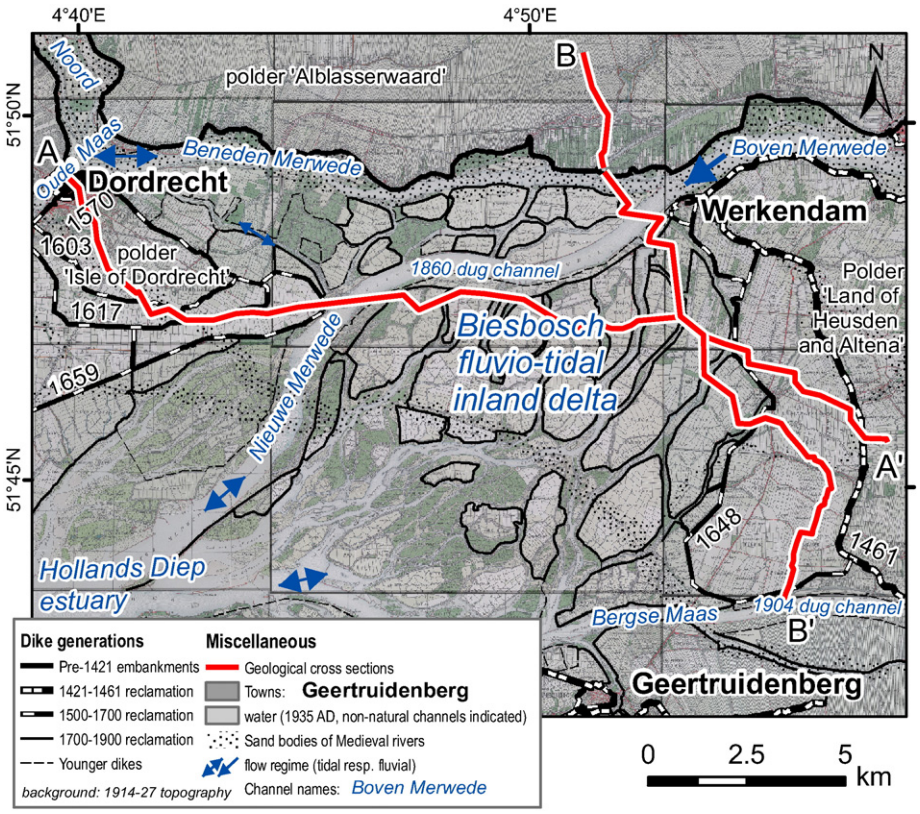

Fig. 2. Study area; channel names and history of reclamation indicated. Locations of geological cross-sections are indicated.

uncertain, such as initial basin depth, tides and past flood regime. These are explored systematically by modelling, which also provides insight on the detailed evolution and the viability of the hypotheses derived from the historical and geological studies. Model results are presented as maps for comparison with historical maps and as synthetic cross-sections for comparison to geological coring transects. Time-varying

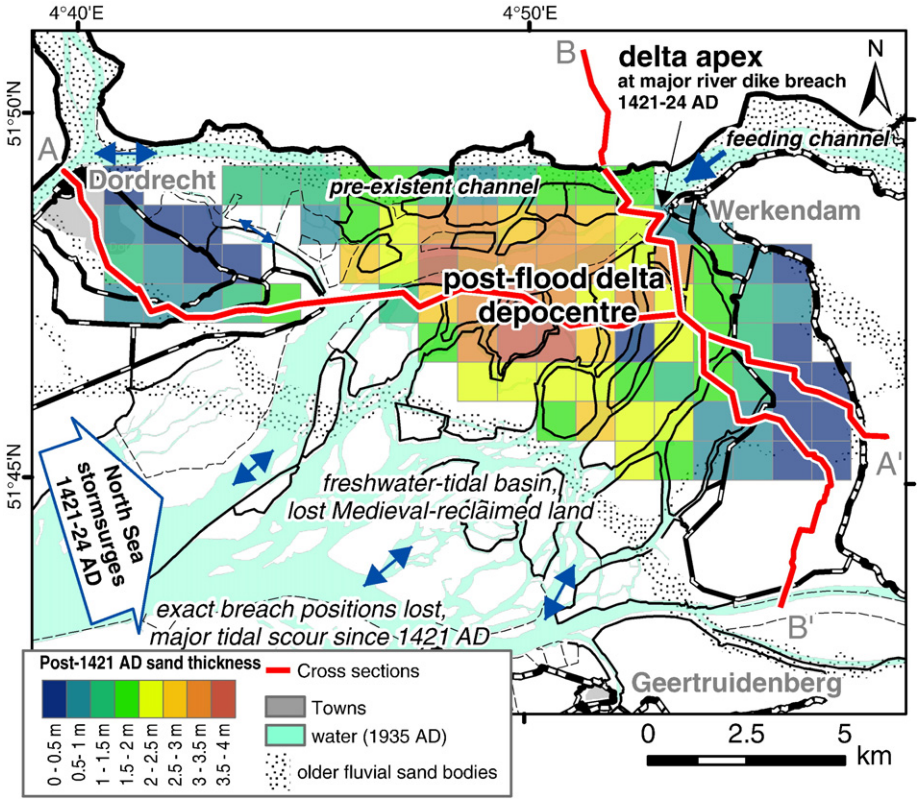

Fig. 3. Thickness of the deltaic splay averaged per kilometre square. Locations of geological cross-sections are indicated. Arrows indicate fluvial and tidal flow directions.

flood water levels are compared for different stages of delta evolution. The modelled and reconstructed sand deposit volumes are also compared to measured modern sediment transport in the Rhine as reported elsewhere (ten Brinke et al., 2001; Kleinhans et al., 2007; Frings and Kleinhans, 2008). Finally, we discuss insights gained from this study and implications for human-induced river diversions. The Appendix contains the complete detailed geological profiles and a movie of the model results.

2. Historical data and analysis

Deltaic splay evolution was interpreted from historical maps, considering meta-information such as their original purpose and geometrical accuracy. Four elements of this study were derived from historical sources: indications as to what extent the inundation was catastrophic, the conditions that led to the inundation, the planimetric evolution of the deltaic splay, and indications for increased river flooding after 1424 AD.

2.1. Sources

Various sources were employed, including studies by historians and archaeologists on the coeval natural and human developments along the rivers of The Netherlands, including floodplain occupation, shipping, military defence and flooding mitigation. Extensive information on historical floodings between 1400 and 1600 AD has been compiled that describes the events leading to the inundation of the study area in detail (Gottschalk, 1975; Buisman, 1996). The development of the upstream river has been documented in maps and written sources with special attention to the upstream bifurcation of the Rhine (in the east of The Netherlands) (van de Ven, 1976; van den Brink, 1998). This includes very detailed and accurate maps and bathymetry of the study area drawn after the frequent 18th and 19th century floodings that led to the digging of the Nieuwe Merwede canal between 1850 and 1885 AD.

Note that the local name of the feeding channel is Boven-Merwede, the pre-1421 AD course is Beneden Merwede ('Merwe'

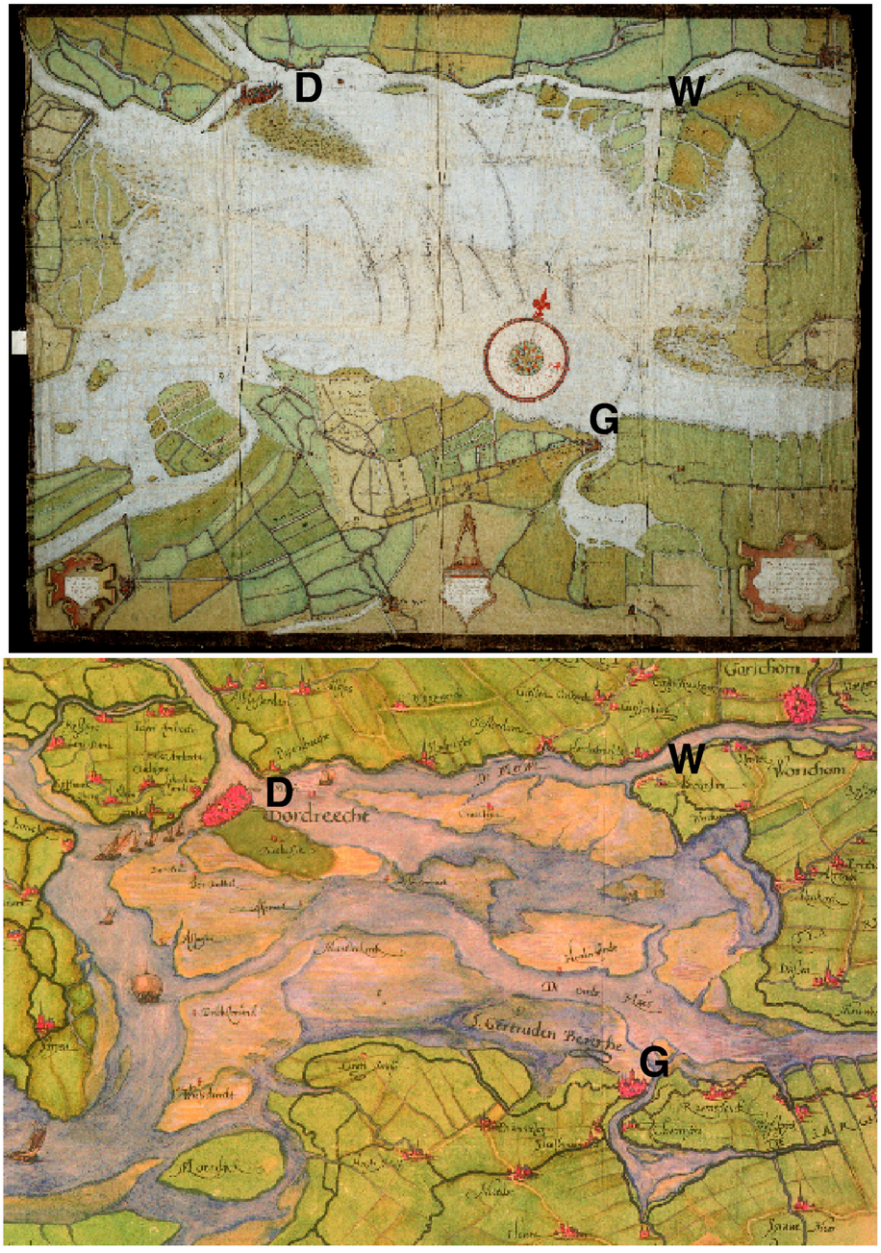

Fig. 4. Historical maps of 1560 (top) and 1568 (bottom). Major cities indicated by D: Dordrecht, W: Werkendam, and G: Geertruidenberg. For scale: the distance between Dordrecht and Werkendam is 15.6 km.

on historical maps) and the present canal, dug through the Biesbosch area in 1850–1885 AD, is the Nieuwe Merwede. The Boven-Merwede is the extension of the major Rhine branch, the river Waal (see Fig. 2).

The following information was derived from four historical maps:

1560 AD (Fig. 4 top) Pieter Sluyter (1560). This map was drawn up accurately for purposes of dividing and taxing the fishing grounds between the Count of Holland (north) and the Prince of Oranje (south) and was commissioned by the latter. Beacons placed in the basin along an east–west line demarcated the border, which followed a Medieval Meuse alluvial ridge (compare main text Fig. 1). The detail in the bars and channels suggest that the map was based on site visits (and, corroborating this interpretation, a sketched map with many notes is also available in the archive). At the apex of the delta, the map also shows spur dikes (Fig. 4 top) built by the city of Dordrecht. These spur dikes, continuously defended with war vessels, were aimed at promoting sediment plug formation in the delta channels, which would force trade ships to continue using the preexisting Merwe channel to Dordrecht where taxes were enforced. Source: inventory number 1895A, Hingman map collection of the National Archive (reproduced with permission) and digitally available as http://beeldbank.nationaalarchief.nl/na:col1:dat511821. Original scale is 1:24,700.

1568 AD (Fig. 4 bottom) Christian Sgrootens (1568). This is a military mapcovering southwestern Netherlands. This map is partly based on a contemporary Zeeland map by Jacob van Deventer, but Sgrootens paid particular attention to the roads, dikes, polders and flooded villages in the study area. The extent of the subaerial tidal flats suggests that the map was drawn for low tide as viewed from the dikes. Hence, smaller channels were not visible and not mapped (in contrast to the 1560 AD map). Source: map 9 of the Atlas Bruxellensis. Facsimile by Canaletto 2007, Alphen aan den Rijn, The Netherlands (reproduced with permission). Original scale is 1:80,000.

1639 AD (Fig. 5) Jacob Aertsz. Colom 1639. This map partly copied maps by other authors drawn between 1621 and 1637 AD. The study area is in the most accurately mapped region. The absence of tidal flats suggests that the map was drawn for Mean High Water when vegetated islands and channels were well visible. Source: Comitatus Hollandiae et Dominii Ultraiectini tabula (Coloms map of Holland and Utrecht). The edition shown here was printed in 1681. Map conservatory of Utrecht University Library, Faculty of Geosciences. Original scale is 1:60,000.

1731 AD Nicolaas Cruquius (1731). The map was designed for planning the digging of the Nieuwe Merwede canal, which was eventually executed a century later (see van den Brink (1998), for extensive analysis of this map). The planning at this time does, nevertheless, prove that flooding upstream of the diversion was problematic. It features the upstream channel (Merwede) and Biesbosch deltaic splay at mean sea level, with levelled cross-sections of bathymetry, information on tides, flood water levels and the datum used. It contains detailed inset maps of a.o. the diversion area where the Merwede bifurcated into the old Merwede and the delta channels. One striking feature is the abundance of vegetation on the bars and annotations regarding countermeasures against vegetation, which was known to increase flood water levels. Source: map conservatory of Utrecht University Library, Faculty of Geosciences (van den Brink, 1998). Scale is 1:10,000.

2.2. Historical reconstruction of the diversion

On 19th November 1421 AD a catastrophic storm surge from the North Sea, the St. Elisabeth Flood, inundated 300 km^2 of Medieval embanked land ('polder') in the densely populated area of Holland (Fig. 3). Tens of villages and valuable agricultural property were flooded. Six weeks later the flooding river Rhine breached the northeastern dike. The inundation was a disaster waiting to happen as civil war and increasing bureaucracy had caused negligence of dike maintenance in preceding decades (Zonneveld, 1960; Gottschalk, 1975). Medieval reclamations had caused the region to become vulnerable to inundation. Peat had been abundantly mined close to the southwestern dikes as a source of income, paradoxically to be used for dike reinforcement (Cleveringa et al., 2004). Also, compaction and

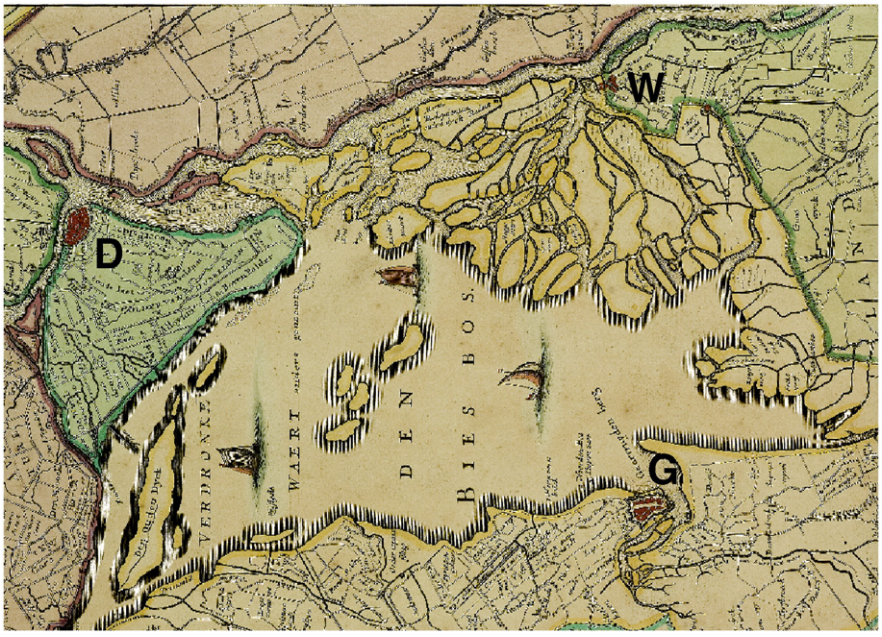

Fig. 5. Historical map of 1639. See Fig. 4.

oxidation of the dewatered peaty topsoil increased dike breach risk. Indeed the polder surface had lowered from above mean sea level to just above ebb tide level due to artificial drainage exploiting low tides.

When the 1421 AD storm surge had breached the weak south-western dike, the Merwede river dike breach could therefore establish a new connection with a southern estuary. Attempted repairs of the dikes were undone by river flooding in 1423–1424 AD and a second storm surge in 1424 AD (Gottschalk, 1975; Buisman, 1996). The lower-most river Rhine diverted into the basin and newly connected to a southern estuary. After 1430 AD the area was given up. Tidal water level variation enhanced scouring of channels and impeded dike repair. In 1461 AD one-third of the area was reclaimed but the western two-thirds remained a freshwater intertidal basin until today (Figs. 2 and 3).

The series of maps show how the post-flood delta developed. It had one main channel and several minor channels intersecting sand bars (Figs. 4–6). The progradation slowed when the delta front reached the old channel belt of the Meuse. By 1639 AD the deltaic splay had prograded about 10 km into the basin, filling most of the north-eastern half to mean sea level (Figs. 4 and 5). The historical map of 1639 AD and Fig. 6 shows that the delta was prograding towards the former Meuse alluvial ridge, which it reached between 1668 and 1700 AD; approximately 260 years after the area had become inundated. The map shows the area that had silted-up above Mean High Water (MHW). Thereafter, transport and sedimentation of sand above MHW in the area was limited (Zonneveld, 1960) as shown by lack of delta progradation in 18th–20th century topographic maps. Sedimentation of sand outside channels after ~1685 is negligible. Within the channels limited sedimentation continued while most of the area trapped fines as upstream estuary and river floodplain.

2.3. Human causes and perception of the catastrophe

A 1676 AD drawing by Houbraken of the post-1421 AD events depicts the catastrophe as a large floodwave that suddenly rushed over the area, drowning as many as 100,000 people according to some sources. This is an overly romantic picture of the true events that nevertheless became the general conception recorded as Dutch history until recently. Various written sources confirm that the 1421–1424 AD inundations were not catastrophic in the sense that a large flood wave suddenly flushed away villages and drowned the inhabitants (Gottschalk, 1975; Buisman, 1996; Hendriks et al., 2004; Cleveringa et al., 2004). A painting (Anonymous) dating back to about 1470 AD shows how the area was evacuated in orderly fashion with time enough to save furniture and cattle. Archaeological investigations in the early 1990s (Hendriks, 1993, 1994) demonstrated that stone buildings in abandoned villages were stripped to their foundations to reuse as building material. However, the consequences of the floods were catastrophic in the sense that much property and arable land, producing grain for Holland, was lost and an unknown number of people, perhaps hundreds, drowned.

There are clear indications in written sources that poor dike maintenance, rather than storm surge magnitude, explains the catastrophe. There are many indications that neither the storm surge nor river flood magnitude in this period were particularly large; however, their frequencies in the 15th century were larger than in the preceding centuries (Gottschalk, 1975; Buisman, 1996). Yet, the 1421 AD storm surge coincided with neap tide, and adjacent areas (northern Netherlands and Flanders) were not affected at all. Dike maintenance in the study area had suffered from political struggles between nobility and laymen (Gottschalk, 1975; Buisman, 1996). Local authorities were aware of this: heavy fines were sometimes dealt out to those who did not maintain the dikes, and imprisonment followed if one could not pay. Nevertheless, a major dike breach had occurred in 1372 AD near Werkendam at the same location where it breached in 1421–1424 AD. A storm surge followed by a second river inundation in 1374 AD worsened the already poor condition of the Merwede southern dike. Several dike breaches along the Meuse River (east of Werkendam-Geertruidenberg) also preceded the 1421–1424 AD catastrophe (Gottschalk, 1975; Buisman, 1996).

3. Geological data and analyses

3.1. Data

Geological data were summarised as (i) interpreted geological sections, and (ii) average thickness per km quadrant and built on established stratigraphic schemes for the Rhine-Meuse delta. We used

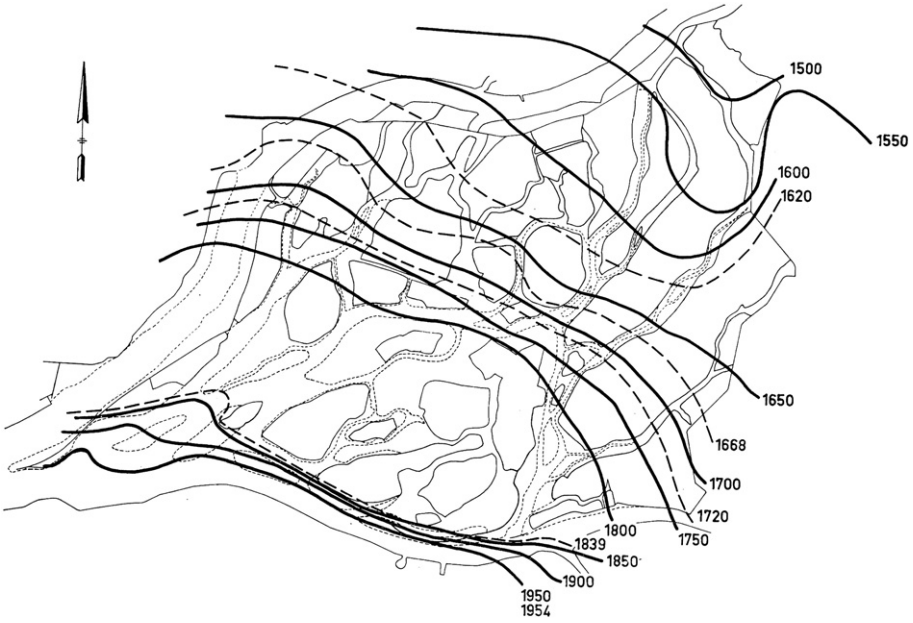

Fig. 6. Progradation of the Biesbosch deltaic splay at MSL derived from historical maps. Measurements along the delta axis will compared to modelled progradation. Zonneveld, 1960.

borehole descriptions from three sources, namely hand coring and mechanical coring in the TNO-DINO database (www.dinoloket.nl) of the Geological Survey of The Netherlands, of hand coring in the UU-LLG database of the faculty of Geosciences (www.geo.uu.nl/fg/palaeogeography) and data of Zonneveld (Zonneveld, 1960). 360 borehole descriptions document the deltaic splay deposits and 171 boreholes make up the sections (Fig. 3).

Fig. 7 shows a section through the Biesbosch area of the composition and the thickness of the deltaic splay deposits (a second, longer section is in the Appendix). Cross-section construction followed methods documented in Gouw and Erkens (2007) and Hijma et al. (2009) and spans the full thickness of the Holocene deltaic thickness. We separated pre-flood from post-flood deposits. Further subdivision and dating is based on established reconstructions and stratigraphic schemes for the Rhine-Meuse delta (Berendsen and Stouthamer, 2000; Gouw and Erkens, 2007). Historical maps and soil mapping (Zonneveld, 1960) were used to detail the top strata between deeper boreholes. The depth of scour features and historical channels matches depths on the 1731 AD historical map.

3.2. Substrate description

The sections allow us to assess degrees of channelized erosion within the delta and differential compaction during delta build up. Furthermore, the cross-sections (Fig. 7) highlight the architectural contrast of the extensive and relative thin sand bodies formed by avulsive deltaic splays (our historical case, formed in two centuries) with narrow distributary ribbon sands encased in extensive clayey and peaty flood-basin deposits (pre-flood channel belts, the dominant architecture for the preceding five millennia).

The deltaic sequence overlies Late Pleistocene and early Holocene fluvial deposits of the joint Rhine-Meuse valley that formed through the area from the end of the last glacial (Busschers et al., 2007) and is capped by a characteristic floodplain clay and coeval isolated inland eolian sand dunes (Törnqvist et al., 1994). The south of the area was outside this valley and has Late Glacial eolian sand sheets draped over terraced older fluvial deposits underlying the delta. The last limb of post-glacial eustatic sea-level rise caused the area to transform from a valley to a tidal flood-basin area, commencing 8000 years ago based on basal peat radiocarbon dating (Hijma et al., 2009). The area became the upper estuary of the river Meuse, accumulating characteristic wood-rich freshwater-tidal subaqueous mud, up to 6500 years ago (Hijma et al., 2009). The permanent inundation of the flood basin is comparable to the post-flood situation in the study area. Thereafter, due to coastal barrier establishment and under much reduced relative sea-level rise, the area became a swampy back-barrier lagoon with extensive peaty flood basins dissected by main Meuse distributaries in the south and minor Rhine distributaries in the north (Berendsen and Stouthamer, 2000). A contrast exists between the architecture resulting from this 'high-stand' situation with relatively stable sea level (apart from slow subsidence) and the underlying 'transgressive' situation with eustatic sea-level rise (strata 0 to 5 m are, respectively, 5 to 10 m below O.D.). A further contrast exists between the deposits from before and after 1421 AD (Fig. 7).

Around 250 BC, a series of avulsions (60–80 km upstream of the study area) caused a main Rhine distributary to divert into the study area. In the first millennium AD this channel became the Merwede main Rhine distributary, that was to be affected by the 1421–1424 AD flood events. Pre-embankment natural overbank deposition by the Merwede left a relative thin clay cover across compaction-prone peat sub-surface only. The surface to the north of the Merwede channel (Albasserwaard) lowered due to stepwise, repeated artificial lowering of the groundwater table since Medieval times (van Asselen et al., 2009).

It is evident that the post-flood sand body geometry is without geological precedent in the study area. However, similar sized splay-shaped sand bodies are known to exist locally to the north of the study area (Hijma et al., 2009), restricted to the transgressive basal part of the Holocene Rhine deltaic wedge at the inland limit of tidal influence (freshwater-tidal or 'perimarine' parts of the delta).

3.3. Sedimentary reconstruction of the fluvio-tidal splay

We identified the 1421 AD event contact and quantified the thickness of sandy and clayey strata above this level. The 1421–1424 AD inundation contact is non-erosive in most places, except along the central axis of the proximal delta and in tidal channels south-west of the delta (Fig. 7). Borehole data show that the delta sand deposits *outside the channels* rest non-erosively on pre-flood deposits. In several archaeological excavations in Dordrecht it was observed that the post-

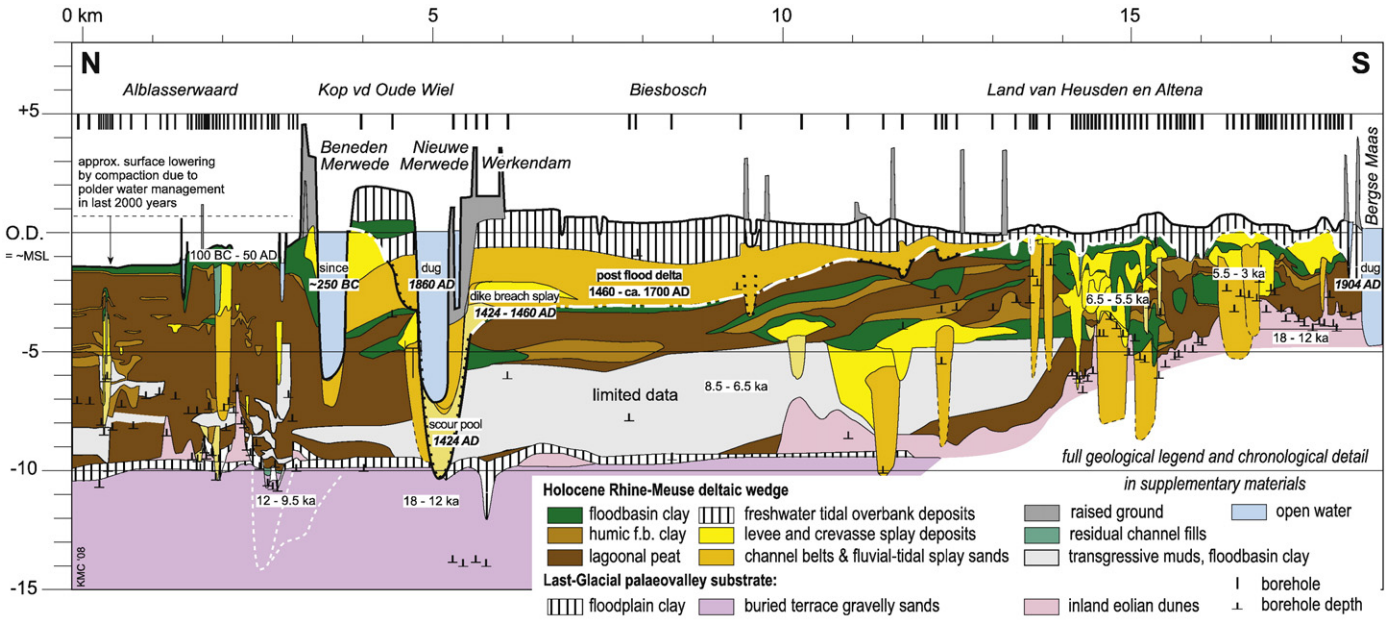

Fig. 7. Geological N–S cross-section through the post-flood deltaic splay (see Fig. 8 and the Appendix for the E–W cross-section).

flood deposit rest on fluvial clay with traces of tillage. This indicates that erosion by the flood has been negligible at these locations. The fluvial clay rests on lagoonal peat in the whole area and can be correlated in the borehole descriptions. Only in the central part of the deltaic splay has this clay bed been fully eroded (Fig. 7). Thus, the post-flood deltaic splay to a large extent buried rather than eroded the pre-1424 AD landscape. The non-erosive nature of the deposits demonstrates that the persistent inundation was the catastrophe for the population rather than the storm impact itself.

The deposits of the St. Elisabeth flood itself are locally preserved under the deltaic splay sand, notably in the NW. The flood deposit is between 1 and 10 cm thick. Abundant juveniles (but no mature specimens) of *Cerastoderma lamarcki* are present in the west and south within this thin flood deposit layer, which indicates short-lived brackish conditions. The post-flood deposits are characterised by the widespread occurrence of adult freshwater molluscs *Bythinia tentaculata* and *Valvata piscinalis*, providing clear evidence for persistent fresh water conditions after 1424 AD, indicative of the predominance of river water.

The post-1421 AD deltaic splay deposit is characterised by bars of medium and fine sand dissected by channels (Fig. 7). The splay sand shows a fining upward trend (medium to fine sand) as expected in a shallow basin. Most of the sand, up to 4 m thick, was deposited proximally along the centre axis of the delta (NE–SW, Fig. 3). The greater thickness of the deposits in the central, proximal part of the area is for a large part caused by syn-sedimentary compaction of the deeper Holocene substrate. Under the weight of accumulating deposits the peaty subsoil compacted, lowering strata up to 3 m. The sands formed between 1421 and 1680 AD and accumulated subtidally, as testified by sedimentology (mud-draped foresets) and historical data.

There is sedimentary evidence for transverse migration of a scouring central channel through the deltaic splay (between 10 and 15 km on section A–A′). The base of subaqueous sandy splay deposits is recognised by the sharp textural contrast with the clayey-peaty buried land surface. Abandoned channels were filled with thin alternating clay and sand layers reflecting tidal water level fluctuations during infilling.

The deltaic sand is capped by 1–3 m of freshwater intertidal floodplain deposits which accumulated mostly after 1600 AD. In the east, progressive reclamations took place in the 18th and 19th century while in the west sediment has continued to accumulate until today. A historical reconstruction compared to the geological cross-section and the modelled geology (see below) is given in Fig. 8.

3.4. Sand budget estimation

To obtain the volume of sand deposits, we used the TNO borehole data that fully penetrated the post-1424 AD deltaic splay. A total of 362 boreholes outside the palaeo-channels and an additional 26 descriptions within channels were available. The latter were not used in the volume calculations, because in-channel deposition may have continued long after 1685 AD. We reconstruct the sand budget for the period of 1424–1685 AD.

For each borehole, the thickness of the delta sand and total thickness of delta deposits were determined. These were averaged per one-km^2 quadrants. The amount of boreholes per quadrant varies from 0 to 20, with lowest density in the area with the thickest

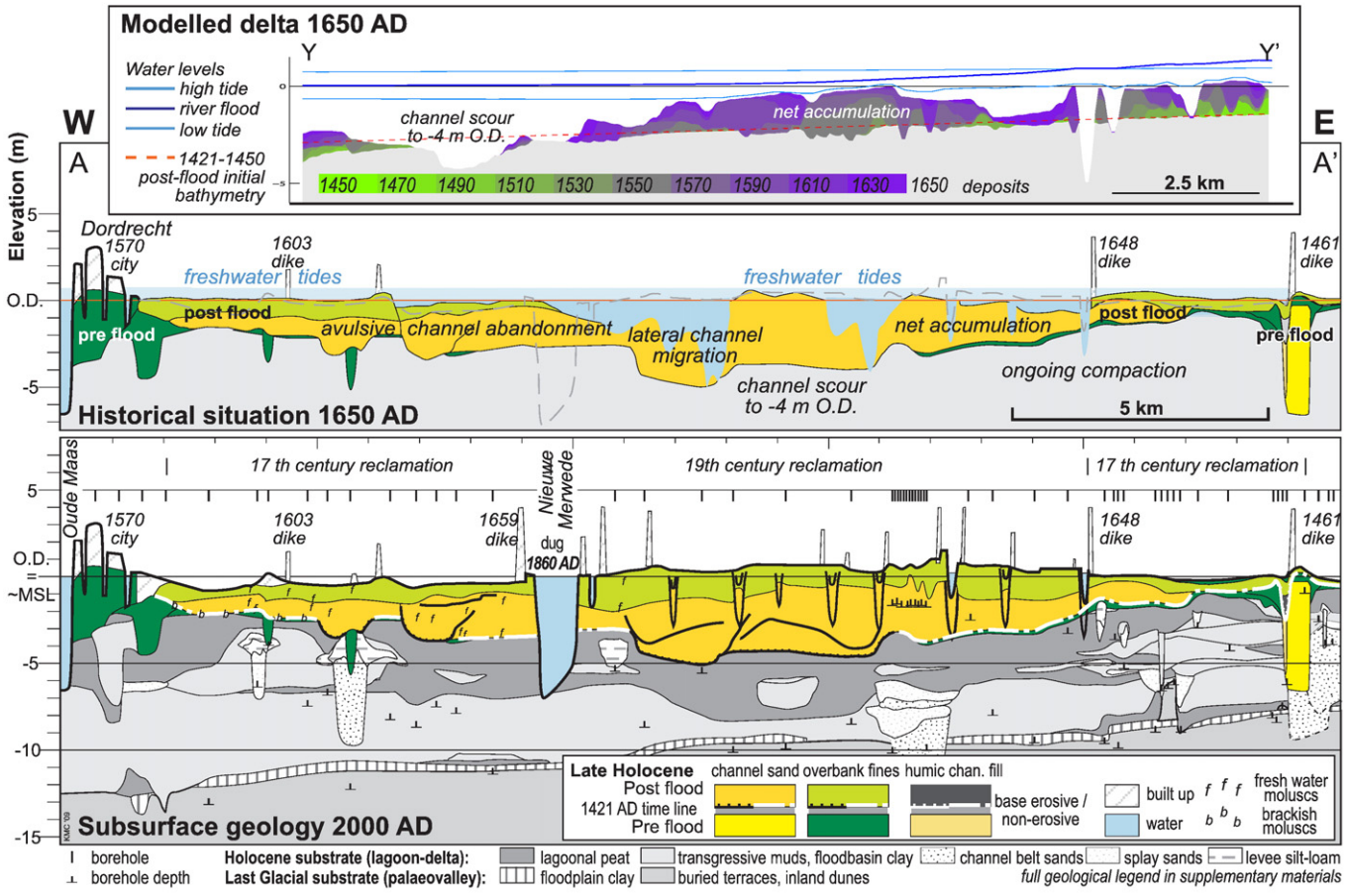

Fig. 8. Modelled, historical and geological E–W cross-sections through the post-flood deltaic splay(see Fig. 2 and Fig. 9 for exact locations of cross-sections; see the Appendix for the detailed E–W geological cross-section).

deposits. In the km quadrants without suitable data (i.e. boreholes not deep and detailed enough), sand thickness was estimated by averaging the four adjacent quadrants. For the quadrants covering only area that was formed before 1685 AD, the averaged thickness equals the volume in million m^3. The volume in quadrants only partly in the 1685 AD area was corrected for the area-percentage that is actually within the area. The total area thus calculated is 85 km^2. All the volumes were then added, yielding an estimate of the total volume of sand in the 1685 AD area.

The thickness of the sandy deltaic splay deposits varies from more than 4 m in the proximal area to less than 0.5 m in the distal parts (Fig. 3). The total volume of sand in the 1424–1685 AD splay is estimated at 151×10^6 m^3, giving a deposition rate of 580,000 m^3/a or 8 mm/a for 260 years. This is a robust and conservative estimate. A less conservative estimate includes the 26 in-channel sand boreholes, increasing the estimated sand volume to 196×10^6 m^3 and an annual rate of 754,000 m^3/a or 10 mm/a. Taking into account that these channels were largely avoided in the mapping programme, the actual sand volume in the area could be larger. However, the historical maps of 1639 AD and 1731 AD indicate that few channels filled in during the period of interest. The upper part of the sand in the central part of the post-flood area may also have been deposited after 1685 AD because of syn-sedimentary compaction of the underlying peat, which would result in a smaller volume than our preferred estimate.

4. Modelling

Idealised scenarios were modelled of an area incorporating the preexisting channel, feeding channel and the evolving deltaic splay. We modelled flow, sediment transport and morphodynamics with a morphodynamic model based on two-dimensional rapidly varied flow equations and a predictor appropriate for bed and suspended transport of sand. Initial bathymetry was schematic and aimed to capture only the most prominent topographic features. Ten scenarios quantify the effects of constant discharge or a natural flood series at the upstream boundary, effect of tides imposed at the downstream boundaries and bracket the likely depth of the basin.

The period between 1461 and 1650 AD is the most interesting to model because the Biesbosch area developed with more or less constant boundary conditions while the splay had not yet prograded up to the central alluvial ridge (former Meuse channel belt). The eastern-most part of the area was reclaimed before 1461 AD and was not considered in the modelling.

4.1. Delft2D model description

We modelled free water surface, flow, sediment transport, erosion and sedimentation with the Delft2D morphodynamic model system (version FLOW3.55.05.779, 10th January, 2008). The model solves the depth-averaged nonlinear shallow-water equations (Lesser et al., 2004). Spiral flow is included through a parameterisation (Struiksma et al., 1985). Bed level change is calculated from gradients in the sum of bedload and suspended bed material sediment transport rates predicted by the van Rijn (1993) predictors (also see Edmonds and Slingerland, 2007). Longitudinal and transverse bed slope effects were applied to the bed load component (Struiksma et al., 1985; Lesser et al., 2004; Kleinhans et al., 2008).

The flow was calculated on a staggered grid by a second order ADI scheme based on the dissipative reduced phase error scheme. Advection of turbulent quantities was computed using a third order upwind ADI scheme in horizontal directions and second order central in the vertical direction. Sediment transport was computed at cell centres; a first-order upwind Lax scheme was used to determine the bed level changes (Lesser et al., 2004).

The time step of the flow was 60 s to ensure numerical stability, and a spin-up period without morphological updating was allowed to stabilise the flow. Sand input at the upstream boundary is kept at the capacity of the flow. Assuming that the flow is not appreciably affected by erosion and sedimentation during a time step, the morphological change in each time step can be multiplied by a factor >1 to predict the morphological evolution more efficiently. The chosen factor was 10 which gave no significant differences with a factor of 1 (no acceleration).

4.2. Specification of model scenarios

We report ten scenarios that bracket the likely boundary conditions and initial conditions and assess the effect of the discharge fluctuations on water levels (Table 1).

In all scenarios, the basin is represented by a rectangular grid with a curvilinear-gridded river channel flowing into the northeast corner and two tidal boundaries in the western corners. The grid size in the basin is 100×50 cells of 200×200 m and in the river is 50×6 cells of 400×100 m. A rectangular grid with the water and sediment entering from a corner of the rectangle provides a critical test of the model, because channels of one grid cell width tend to follow 0° and 90° orientations whereas the main axis of the deltaic splay is at 45°.

The idealised initial bathymetry captures the general gradient of the area, the pre-flood levee of the abandoned Rhine branch and the channel-belt ridge in the basin. Control runs without the dike breach (called 'no basin' hereafter, Table 1) confirmed that the initial channel morphology is reasonably in equilibrium. Overall initial basin depth cannot accurately be recovered from geological data because the soil below the flood deposit has compacted. The initial basin depth was therefore chosen at 4 m (measured in the shallowest part in the north-eastern corner; called 'deep' hereafter) and 2 m ('shallow') below MSL while upstream and old channel bathymetry was kept the same between runs. The initial bed of the upstream channel was plane and had a gradient of 1×10^{-4} m/m. The bed sediment size was 0.25 mm.

The hydraulic roughness had a constant Chézy value of $C=45$. This value is based on calibrated model experience in the river Rhine. Given the typical water depth, a Nikuradse roughness length of 0.15 m could have been used instead. The effect of choosing a constant Chézy number instead of a constant Nikuradse roughness length is limited (Lesser et al., 2004; Kleinhans et al., 2008) and would not change our general morphological results and trends in water level change. Effects of vegetation on the shallower areas will be discussed later with the predicted flood levels.

The imposed boundary conditions are upstream flow discharge and downstream water levels. Until the 1960s, the observed tidal range at the downstream boundary of the basin was about 2.1 m (Weerts et al., 2005). The downstream water levels were either specified at constant mean sea level or as tidal components M2 and O1 with a phase difference derived from present-day measurements. The applied M2 and O1 amplitudes are 0.8 m and 0.15 m; the phase lag of the northwestern boundary on the southwestern boundary is 3.5 and

Table 1
Model scenarios. The preferred scenario, in hindcast, is indicated.

Scenario	Name	Northeastern basin depth	Downstream boundary
1	No basin, river flow only	Preexisting channel only	MSL
2	No basin, river and tides	Preexisting channel only	2.1 m tidal range
3	Shallow basin, river flow only	2 m	MSL
4	Shallow basin, river and tides	2 m, *preferred*	2.1 m tidal range
5	Deep basin, river only	4 m	MSL
6	Deep basin, river and tides	4 m	2.1 m tidal range
7	No basin, floods	Preexisting channel only	MSL
8	Shallow basin, floods	On #4 after 10 years	MSL
9	Shallow basin, floods	On #4 after 50 years	MSL
10	Shallow basin, floods	On #4 after 200 years	MSL

7.15 h, respectively. Feeding channel discharge was set constant at 1600 m^3/s. This yields the same amount of sediment transport in the upstream channel as, on average, for the complete discharge record of the past century (Kleinhans et al., 2008).

To assess flood water level change due to the deltaic splay progradation, a time series of discharge of the Rhine between 1981 and 2000 was applied to modelled morphology of the shallow basin case with tides after 10, 50 and 200 years and to the case without basin (scenarios 7–10). The downstream boundary condition for these runs was constant water level. The width-averaged water level just upstream of the bifurcation for these time steps is compared so that the relative effect of the evolving deltaic splay on the water levels is assessed as far away from the upstream model boundary as possible.

The model simplifies reality in several ways, most importantly a simplified initial bathymetry, as detailed data is not available. The advantage of this simplification is that the interesting autogenic morphodynamics are entirely due to the flow and sediment dynamics and not determined strongly by the initial conditions. Silt and clay sediment were not incorporated in the model. Although fines were imported from both the river and the Hollands Diep estuary, their contribution to the deltaic splay is minor. Furthermore the Rhine river has an equal annual budget of sand (gravel upstream) and fines, while the fines mostly deposit further downstream in the estuaries (ten Brinke et al., 2001).

4.3. Modelling results

4.3.1. Modelled deltaic splay planform evolution

A deltaic splay forms in all model runs except those without a basin (Figs. 9–11). Dissective distributary channels avulse over the splay. The channels are one to two grid cells wide, which indicates that the grid is relatively coarse, but a twice finer grid would take an inhibitive four-times longer computation time and the main focus of this paper is sediment budget and large-scale features.

Sand is mainly deposited proximally as bars between the channels; as prograding mouth bars at the splay front; and as plug bars filling channels after local avulsion. The progradation of mouth bars reduces the upstream channel gradient. This forces sedimentation to propagate upstream, causing new avulsion further upstream because flood water levels rise due to the sedimentation.

The progradation rate of the deltaic splay depends on the depth of the tidal basin and on the sediment input from the river. From geometry it follows that, for a constant sediment input, the deltaic splay volume increase is constant, which for a radial feature leads to splay front progradation decreasing with the square-root of time (Fig. 12) in agreement with the progradation derived from historical maps. The upstream channel only had a few cm sedimentation over 200 years and is therefore considered to be in equilibrium.

Scenarios with tidal flow show that the deltaic splay progrades considerably faster and aggrades higher compared to scenarios with constant river discharge only (Fig. 12). This is due to ebb-currents and tidal water level variation. The effect of net tidal currents combined with the east-to-west ridge and tidal asymmetry in the shallow basin scenario leads to a significantly faster progradation of the northern splay rim (Fig. 12B) in agreement with the historical maps.

Despite the coarse grid, a rich morphology develops in the model in qualitative agreement with historical maps. In particular, smaller, southward directed channels appear in the eastern part of the deltaic splay, whereas larger (and more) westward directed channels appear over most of the splay (compare Fig. 5 with Fig. 10). This agrees with the historical map and only occurs in the preferred scenario, presumably because of the tidal flow conditions. Furthermore, a new breach in the levee develops in the northwestern corner. The southwestern corner is scoured by the tides, but this is probably exaggerated in the model as no influx of sediment is specified that would cause sedimentation during ebb flow. Alternating bars develop in the abandoning channel.

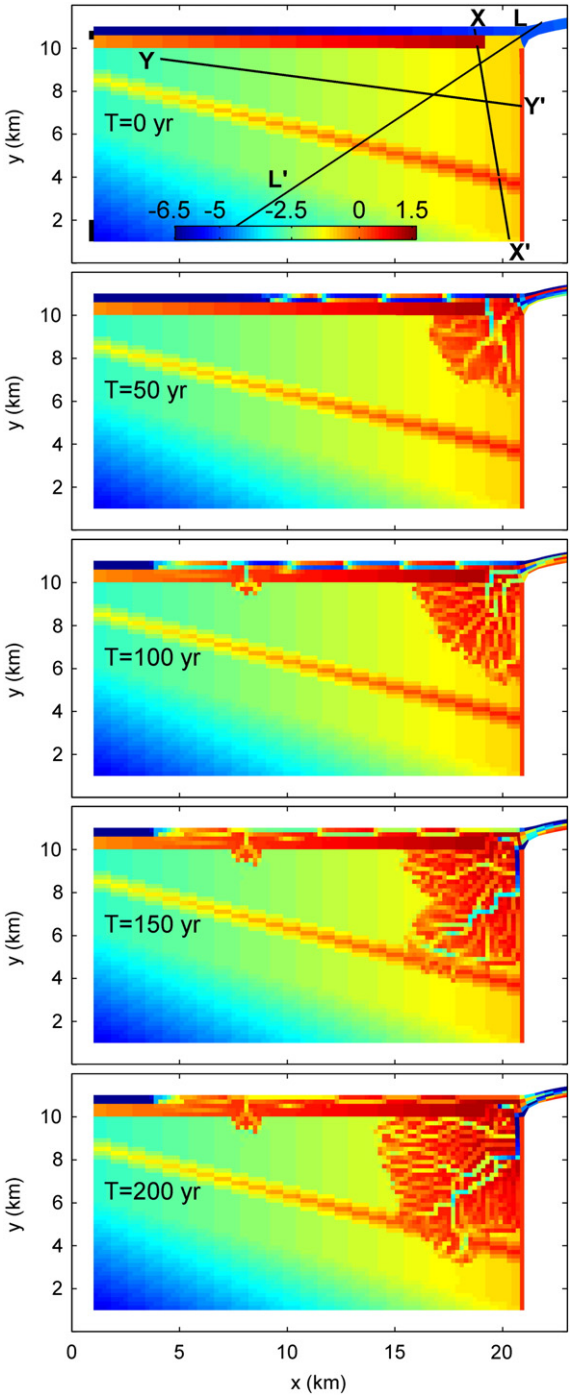

Fig. 9. Modelled bed surface for a shallow basin with fluvial current only (m +/− O.D., scenario 3). Model domain extends 20 km into feeding channel (not shown). Imposed downstream water level boundaries indicated with bold lines in $T=0$ a panel.

4.3.2. Modelled geology and sand budget

Synthetic geological sections are derived from the preferred scenario model results (Fig. 13), showing erosion into older subsoil and the age of deposits preserved after 200 years. In the most proximal part of the deltaic splay where the river flow focusses through the gap into the basin, considerable erosion is seen, but over most of the original basin floor no erosion occurred. Migrating channels create relatively wide channel belts that are infilled gradually as a result of avulsion while other channels become active, in agreement with the geological and historical data (Fig. 8).

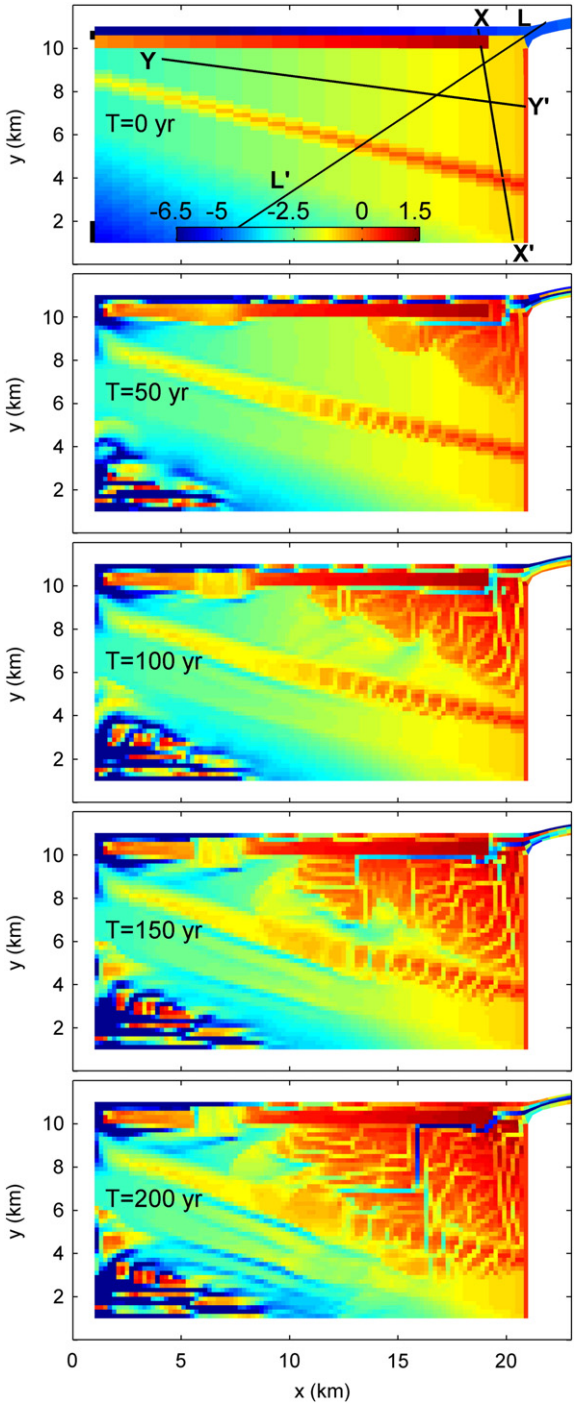

Fig. 10. Modelled bed surface for a shallow basin with tides (preferred scenario 4). Thin black lines indicate locations of synthetic geological cross-sections (Fig. 13). Legend as in Fig. 9. Movies in the Appendix.

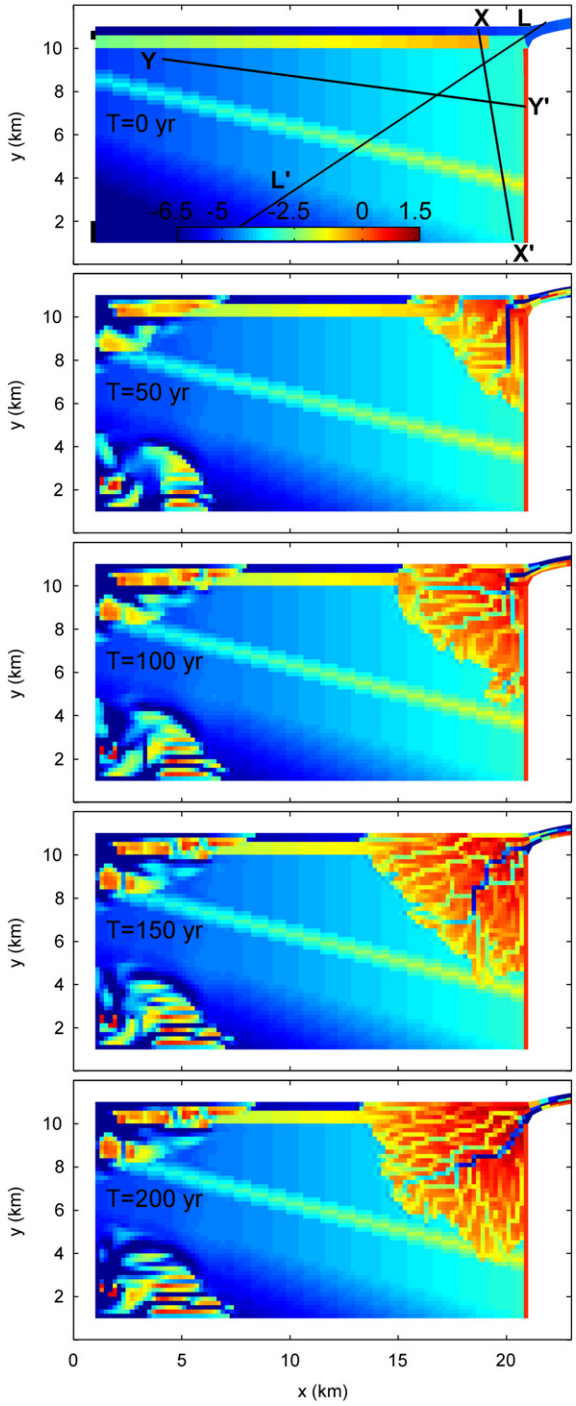

Fig. 11. Modelled bed surface for a deep basin with tides (scenario 6). Legend as in Fig. 9.

Modelled sand deposition in the deltaic splay is $2.6–5.3 \times 10^5$ m^3/a for different scenarios which, considering the usual uncertainty of sediment transport prediction, is in good agreement with the sediment budget reconstructed from the cores and the present day measured transport rate in the feeding channel (Table 2). The rate of deposition in the splay is about 1.5 times as much for the deep basin as for the shallow basin. The presence of tides also increases the fluvial sand import about 1.5 times. The feeding channel erodes considerably in the first decades but afterwards had net sedimentation since the preexisting channel had filled in and an initial splay had formed. Our results imply that the feeding channel effectively diverted its entire bed sediment load into the basin.

4.3.3. Modelled bifurcation evolution and flood water levels

The preexisting channel becomes plugged up within decades in all model scenarios (Fig. 14). This happened due to the gradient advantage induced by the flow expansion onto the flood basin as well as the tidal amplitude, and it happened despite the position of its entrance at the outer-bend of the feeding channel that would favour opening (Kleinhans et al., 2008). The near-closure of the preexisting channel is gradual for the river flow cases but much more rapid for the river-and-tidal cases (scenarios 3–6). For the deep basins, the preexisting channel was filled in by a much shorter but higher bar in the first decade so that the entire discharge went through the Biesbosch area (Fig. 14, Table 2). For the shallow basins, the old

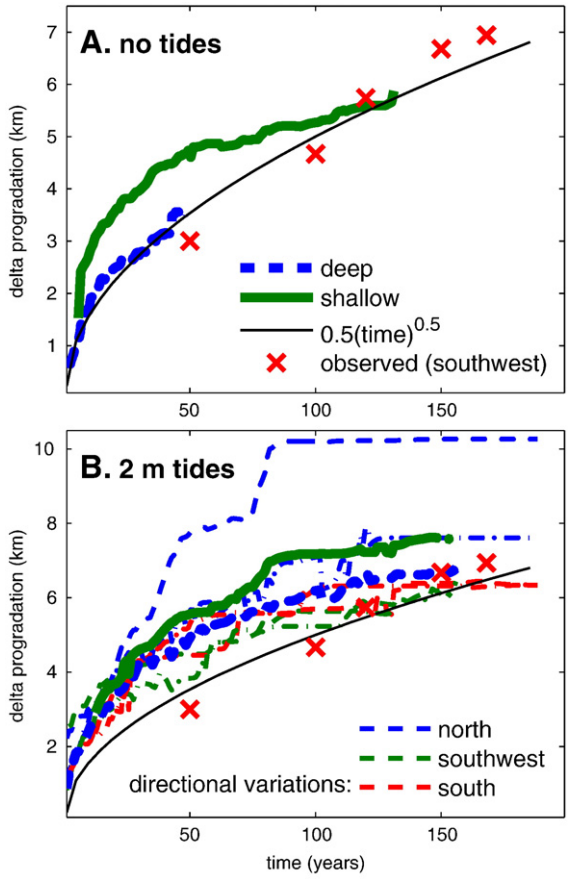

Fig. 12. Modelled and observed (Fig. 6) progradation for non-tidal (A) and tidal (B) scenarios. For the shallow basin with tides the progradations along E–W, NE–SW and N–S lines is given as well to illustrate deltaic splay asymmetry and avulsive behaviour.

channel filled up more slowly because friction for the fluvial and tidal discharge became significantly larger than in the deep basins, so that more flow went through the old channel. This is attested by the morphodynamics at the Meuse channel belt in the shallow basin case, indicating high velocities with significant friction at the bed. Alternating bars developed as in the scenarios without the basin. Systematic annual dredging of the old channel (Beneden Merwede) only took place since about 1800 AD when steamboats became available. The shallow basin scenario with tides is in better agreement with the measured progradation rate and channel orientations (assessed by eye) on the historical map.

Upstream water levels were affected by the widened and shallowing cross-sectional area as both the old channel and the new course were filling in. The maximum modelled flood water level just upstream of the bifurcation increases from 0.25 m after 50 formative years to about 0.7 m after 200 years (Fig. 15). The modelled flood increases are minimum estimates because abundant vegetation on top of the shallowing splay, causing additional hydraulic resistance, was not modelled. The rise demonstrates that flood water levels, and hence inundation frequency, increased with shallowing of both the infilling preexisting channel and the emerging splay, again in agreement with historical records (Gottschalk, 1975).

Summarising, the model scenario that matches historical and geological data best is that with a shallow basin depth with tides (scenario 4). Still, in reality the deltaic splay surface subsided when the subsoil compacted under the increasing loading by the splay. Compaction will not affect our general conclusions, however. The deep and shallow basin scenarios bracket realistic sediment budgets and produce progradation rates in agreement with the historical maps. Besides compaction, other sources of underestimation in the pace of sedimentation in scenario 4 by the model may be found in large uncertainties of sediment transport predictors (van Rijn, 1993), a possible underestimation of the upstream channel gradient or errors in the reconstructed volume, and uncertainty of the feeding channel discharge in the 1450–1650 AD period.

5. Discussion

Our site-specific results are summarised as follows. The development of the deltaic splay following river diversion can be seen in Figs. 6, 10 and 12. A large area of subrecent fluvial plain, vulnerable due to human actions and negligence, was simultaneously inundated from the river and from the sea which led to catastrophic land loss. The river connected to an estuary through the inundated area. Hence, it attracted so much flow that it trapped the river's entire sediment load. As a result the inundated area filled up at the fastest possible rate. Thus the splay-formation process presents a way in which delta river branches heal their scars after major inundation incidents. Nevertheless it took centuries before a considerable area emerged above mean sea level and could be reclaimed, with subsoil compaction as a retarding factor (Fig. 7). The inland deltaic splay formed mostly non-erosively through mouth bar formation and diversions of the splay channels, which on average prograded the splay front radially (Figs. 6, 10 and 12). Meanwhile, the old river channel infilled, a process explained morphodynamically by Kleinhans et al. (2008), so that both old and new course effectively resisted flood discharge. This caused higher flood water levels upstream of the diversion area (Fig. 15) that may have repeatedly led to dike breaches over tens of km upstream for centuries.

The results elucidate under which conditions avulsive inland deltaic splay formation is fast paced or when new channels and river mouths are initiated in the downstream parts of deltaic plains: this depends on the balance of downstream flow connection effects and downstream sediment-trapping effects. Until now, elaboration of necessary and sufficient conditions for avulsion concentrated on upstream mechanisms (Smith et al., 1989; Wang et al., 1995; Slingerland and Smith, 1998; Bolla Pittaluga et al., 2003; Kleinhans et al., 2008) but our results shows that the downstream potential for flood conveyance, or downstream flow attraction by tides, strongly enhance the possibility for fast and full avulsion because the energy gradient is increased. These conditions are found particularly where levees breach and flow and sediment diverts into a permanently inundated tidal flood basin, such as in the downstream parts of major deltas. In such circumstances, sandy splays grow in volume much faster than the sandy channel-belt bodies that are their upstream feeders and appear much more effective in trapping sand than crevasse splays developing in shallower, only seasonally inundated flood basins that characterise upstream parts of deltas (Smith et al., 1989; Stouthamer and Berendsen, 2000; Makaske et al., 2002). Our case demonstrates that splay formation may attract nearly the entire bed sediment budget of the river when the inundated flood basin connects to a downstream fluvial channel or tidal estuary. The presence of a downstream flow connection increases the likelyhood of successful lower-delta avulsions. Conversely, avulsion into a small or enclosed basin is less likely to be successful.

Of equal importance but opposing the connection effect is the increased sediment-trapping capacity of the permanently inundated flood basin, which blocks the river flow and the tides to such extent that the avulsion may fail. Upstream flood water levels increased as the deltaic splay built out and the former channel infilled. In agreement with historical data, the flood conveyance of the combined former channel and flood basin reduced relative to that of the former channel before the diversion. The nonlinear reduction of sediment transport led to effective trapping of the entire budget of the river in the diversion area. The shallowing channels must increasingly have trapped large woody debris in natural rivers, but vegetation was removed by inhabitants in our study area. Furthermore, historical

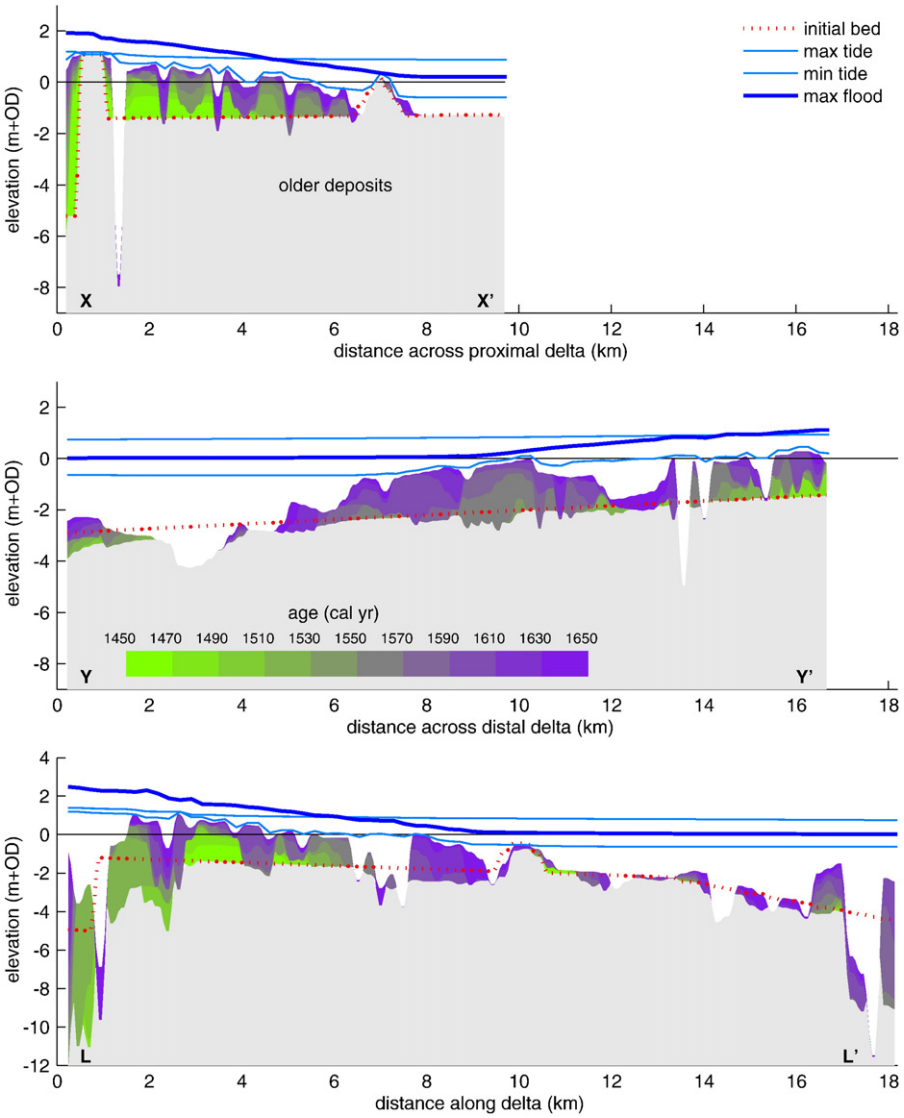

Fig. 13. Synthetic geological sections along and across the tide-generated deltaic splay in the shallow basin (preferred scenario 4). Tidal range and maximum flood water levels are indicated. Section Y–Y′ is also included in Fig. 8.

records show frequent ice dams in this period (the beginning of the Little Ice Age) (Gottschalk, 1975; Buisman, 1996; Glaser and Stangl, 2004), which alone could have increased flood frequency but must have been exacerbated by the shallowing flow in both channels downstream of the bifurcation.

This raises the question whether increased upstream flood levels could induce an upstream-moving avulsion sequence as predicted by Mackey and Bridge (1995), and observed by Stouthamer and Berendsen (2007) for the Holocene Rhine delta and by Hoyal and Sheets (2009) in experiments. On a small scale, this is observed on the modelled deltaic splay following mouth bar sedimentation. On a large scale, upstream avulsions did not take place in the human-influenced fluvial plain of the Rhine but many dike breaches did, indicating that in the absence of human interference avulsion could have taken place.

Our results elucidate a contrast between upstream fluvial avulsion and downstream tidal-river avulsion. Shallow fluvial floodplains foster thin crevasse splays that are often abandoned but sometimes grow out into a full avulsion. In the deeper fluvio-tidal basins the attraction of flow by downstream tidal channels enhances the probability of full avulsion, but the deeper basins are also more efficient sediment traps. This applies to the modern high-stand situation, but applies equally to preceding transgressive situations from when these modern deltas came into existence (Stanley and Warne, 1994), of which the muddy upper-estuarine deposits at depth (Fig. 7) include bay-head deltas Hijma et al. (2009) and lake-filling crevasse splays (Bos et al., 2009) just north of our study area at the inland limit of tidal influence.

These new insights, in particular the upstream flooding and the factors determining the pace of sedimentation, are also relevant for modern applications. It has been suggested to artificially create controlled diversions of large river channels from the main river aimed at mitigating storm surge inundation risk in subsiding areas such as the Mississippi delta, Louisiana (Florsheim and Mount, 2002; Reed and Wilson, 2004; Day et al., 2007). Similarly, such diversions have been used to reduce river flood risk in preexisting channels, e.g., in the Huanghe delta (Yellow River, China) (Syvitski and Saito, 2007). Indeed, new deltaic bodies steadily improve delta land protection against the sea, controlled by sediment load, mean sea level and subsoil compaction, but this takes decades to centuries even if they capture the entire sand budget of the river. Moreover, such measures must account, perhaps by engineered structures, for unbalanced river bifurcations (Kleinhans et al., 2008), and for long periods with increased flooding risks in the feeding channel, the preexisting channel and the recovering land. In the modern situation in The

Table 2
Modelled sediment deposition rates ($\times 10^5$ m^3/a) in the deltaic splay, the deltaic channels, the old channel and the upstream channel. Negative numbers indicate erosion.

#	Name	Deltaic splay	Deltaic channels	Old channel	Upstream channel
Averaged over first 50 years					
3	Shallow basin, river flow only	2.6	0.2	2.4	−0.6
4	Shallow basin, river and tides	4.1	1.3	2.2	−0.8
5	Deep basin, river only	3.7	0.1	2.2	−1.1
6	Deep basin, river and tides	5.3	0.3	1.9	−1.2
Averaged over 200 years					
3	Shallow basin, river flow only	2.2	0.3	1.4	0.4
4	Shallow basin, river and tides	3.4	0.8	1.3	0.3
6	Deep basin, river and tides	4.4	0.2	1.1	0.3
Reference values					
	Geological reconstruction	5.8	1.7		
	Present-day rate (1970–2000)	6			

Netherlands a 0.75–1.0 m rise in water level would have to be compensated by raising hundreds of kilometres of dikes, which would cost of the order of a billion Euros.

6. Conclusions

This study reports a detailed reconstruction and explanation of causes, dynamics, sedimentation pace and upstream flood water levels for a river diversion into a tidal flood basin. Key aspects derived from historical and geological data were successfully reproduced by modelling. The main conclusions are:

- The ultimate causes of the 1421–1424 AD inundations that led to the river diversion were poorly maintained dikes and rapid compaction of the peaty subsoil due to human action and negligence. The avulsion was successful and had dramatic effects because the freshwater-tidal flood basin became connected to a downstream estuary, so that a direct connection to the sea was established.
- As a result, an inland deltaic splay formed that captured the entire sand budget of the river for two centuries. Sedimentation proceeded by cycles of mouth bar formation, channel gradient reduction, backward sedimentation, local upstream avulsion and renewed mouth bar build up downstream of the new outlet. Channel migration was limited. The deltaic splay deposited non-erosively on the subsoil, except at the deeper proximal channels.
- The bifurcation of the feeder channel, old course and inland deltaic splay was unstable and the former river channel rapidly infilled and was nearly abandoned within decades. Simultaneous deltaic splay build up and old channel infilling caused higher flood water levels upstream of the diversion for two centuries.
- The balance of the downstream flow connection and tidal attraction and the downstream flow blocking by sediment trapping determines whether inland bay-head deltas form or whether new channels and river mouths form. Full and fast avulsion is more likely in long flood basins with tidal water level fluctuations. On the other hand, deeper tidal fluvial flood basins are more efficient sediment traps than shallower fluvial floodplains, leading to eventual blocking of flow.
- The rapid sedimentation at the inland deltaic splay and the abandoning channel causes upstream flooding and may cause upstream sedimentation. This has ramifications for human-induced river diversions aimed at reducing flood and inundation risk. Furthermore, it potentially explains upstream-moving sequences of avulsion.

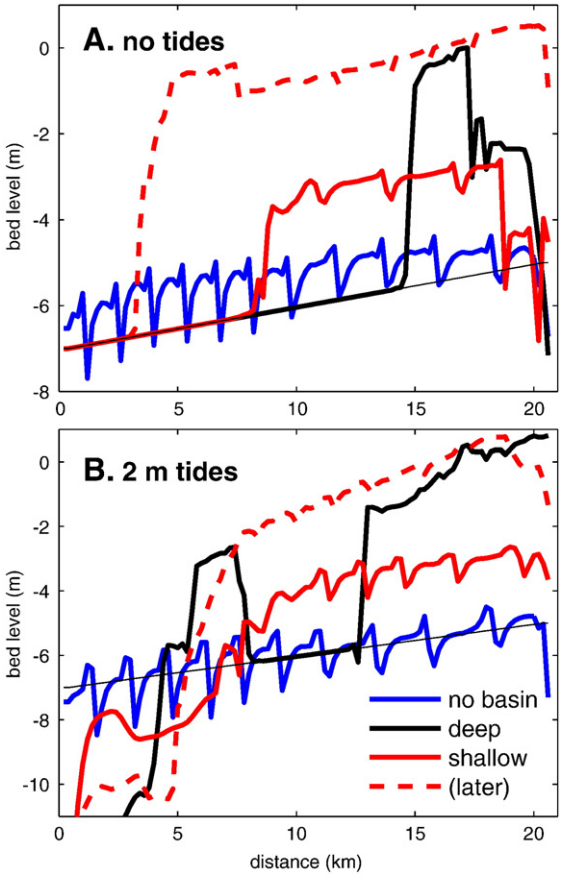

Fig. 14. Bed elevation (width-averaged) of the preexisting channel after 50 years (dashed lines: 200 years) for the current and tide scenarios. Cases without a basin shows alternating bars. Cases with shallow and deep basins and a deep basin show rapid infilling, indicating a highly dynamic and asymmetrical bifurcation.

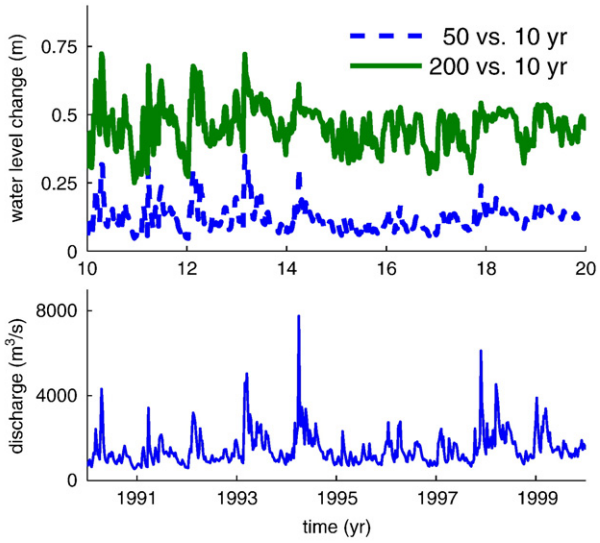

Fig. 15. Modelled water level *increase* relative to initial situation (0 year) (top) after 50 and 200 years just upstream of deltaic splay apex (only last decade of flow discharge shown to exclude adaptation effects in first 5 years).

Acknowledgements

Four reviewers provided comments that helped to improve the paper. Discussions on map sources and accuracy with Marco van Egmond (map conservator, Utrecht University Library) and Valentine Wikaart (conservator, Biesboschmuseum) are gratefully acknowledged. Jeroen Schokker (TNO/Deltares) is acknowledged for making extensive

borehole data available. J. Hendriks (Dordrecht Archaeology) is acknowledged for initiating geological research in the study area. MGK was supported by The Netherlands Organisation for Scientific Research (NWO) (grant ALW-VENI-863.04.016). KMC was supported by the Utrecht Centre of Geosciences. The authors contributed in the following proportions to conception and design, historical and geological reconstruction, modelling, analysis and conclusions, and manuscript preparation: MGK (60, 10, 90, 40, 60%), HJTW (30, 60, 0, 30, 10%) and KMC (10, 30, 10, 30, 30%). The Appendix contains detailed geological cross-sections and a movie of the preferred model scenario.

Appendix A. Supplementary data

Supplementary data associated with this article can be found, in the online version, at doi:10.1016/j.geomorph.2009.12.009.

References

Berendsen, H., 1998. Birds-eye view of the Rhine-Meuse delta (The Netherlands). Journal of Coastal Research 14, 740–752.
Berendsen, H., Stouthamer, E., 2000. Late Weichselian and Holocene palaeogeography of the Rhine-Meuse delta, The Netherlands. Palaeogeography, Palaeoclimatology, Palaeoecology 161, 311–335.
Bolla Pittaluga, M., Repetto, R., Tubino, M., 2003. Channel bifurcation in braided rivers: equilibrium configurations and stability. Water Resources Research 39, 1046.
Bos, I., Feiken, H., Bunnik, F., Schokker, J., 2009. Influence of organics and clastic lake fills on distributary channel processes in the distal Rhine-Meuse delta (The Netherlands). Palaeogeography, Palaeoclimatology, Palaeoecology 284 (3–4), 355–374. doi:10.1016/j.palaeo.2009.10.017.
Buisman, J., 1996. Thousand years of weather, wind and water in the low countries. Part 2: 1300–1450. van Wijnen, Franeker, The Netherlands.
Busschers, F., Kasse, C., van Balen, R., Vandenberghe, J., Cohen, K., Weerts, H., Wallinga, J., Johns, C., Cleveringa, P., Bunnik, F., 2007. Late Pleistocene evolution of the Rhine-Meuse system in the southern North Sea basin: imprints of climate change, sea-level oscillation and glacio-isostacy. Quaternary Science Reviews 26, 3216–3248.
Cleveringa, P., Hendriks, J., van Beurden, L., Weerts, H., van Smeerdijk, D., Meijer, T., de Wolf, H., Paalman, D., 2004. 'So grot overvlot der watere...' Een bijdrage aan het moderne multidisciplinaire onderzoek naar de St. Elisabethsvloed en de periode die daaraan vooraf ging. Holland Historisch Tijdschrift 36, 162–180.
Day, J., Boesch, D., Clairain, E., Kemp, G., Laska, S., Mitsch, W., Orth, K., Mashriqui, H., Reed, D., Shabman, L., Simenstad, C., Streever, B., Twilley, R., Watson, C., Wells, J., Whigham, D., 2007. Restoration of the Mississippi Delta: lessons from Hurricanes Katrina and Rita. Science 315 (5819), 1679–1684.
Edmonds, D., Slingerland, R., 2007. Mechanics of river mouth bar formation: implications for the morphodynamics of delta distributary networks. Journal of Geophysical Research 112, F02034.
Florsheim, J., Mount, J., 2002. Restoration of floodplain topography by sand-splay complex formation in response to intentional levee breaches, Lower Cosumnes River, California. Geomorphology 44, 67–94.
Frings, R.M., Kleinhans, M.G., 2008. Complex variations in sediment transport at three large river bifurcations during discharge waves in the river Rhine. Sedimentology 55, 1145–1171.
Glaser, R., Stangl, H., 2004. Climate and floods in Central Europe since AD 1000: data, methods, results and consequences. Surveys in Geophysics 25, 485–510.
Gottschalk, M.K.E., 1975. Storm Surges and River Floods in The Netherlands I (the period 1400–1600). van Gorcum, Assen, The Netherlands.
Gouw, M., Erkens, G., 2007. Architecture of the Holocene Rhine-Meuse delta (The Netherlands) — a result of changing external controls. Netherlands Journal of Geosciences 86, 23–54.
Hendriks, J., 1993. Hernieuwd onderzoek aan Kasteel Muilwijk (I): de Voorburcht. Terra Incognita 1-I, 11–15.
Hendriks, J., 1994. Hernieuwd onderzoek aan Kasteel Muilwijk (II): de Hoofdburcht. Terra Incognita 2-I, 23–29.
Hendriks, J., Cleveringa, P., van Beurden, L., Weerts, H., Meijer, T., van Smeerdijk, D., Paalman, D., 2004. 'Dar vordrunken 16 schone kerspele...' Introductie op het moderne interdisciplinaire onderzoek naar de St. Elisabethsvloeden, 1421–1424. Westerheem 53, 94–111.
Hijma, M., Cohen, K.M., Hoffmann, G., van der Spek, A., Stouthamer, E., 2009. From river valley to estuary: the evolution of the Rhine mouth in the early to middle Holocene (western Netherlands, Rhine-Meuse delta). Netherlands Journal of Geosciences 88, 13–53.
Hoyal, D., Sheets, B., 2009. Morphodynamic evolution of experimental cohesive deltas. Journal of Geophysical Research 114, F02009.
Kleinhans, M.G., Wilbers, A., ten Brinke, W., 2007. Opposite hysteresis of sand and gravel transport up- and downstream of a bifurcation during a flood in the River Rhine, The Netherlands. Netherlands Journal of Geosciences 86, 273–285.
Kleinhans, M.G., Jagers, H., Mosselman, E., Sloff, C., 2008. Bifurcation dynamics and avulsion duration in meandering rivers by one-dimensional and three-dimensional models. Water Resources Research 44, W08454. doi:10.1029/2007WR005912.
Lesser, G.R., Roelvink, J.A., van Kester, J.A.T.M., Stelling, G., 2004. Development and validation of a three-dimensional morphological model. Journal of Coastal Engineering 51, 883–915.
Mackey, S., Bridge, J., 1995. Three-dimensional model of alluvial stratigraphy: theory and application. Journal of Sedimentary Research B65, 7–31.
Makaske, B., Smith, D., Berendsen, H., 2002. Avulsions, channel evolution and floodplain sedimentation rates of the anastomosing upper Columbia River, British Columbia, Canada. Sedimentology 49, 1049–1071.
Reed, D., Wilson, L., 2004. Coast 2050: a new approach to restoration of Louisiana coastal wetlands. Physical Geography 25, 4–21.
Slingerland, R., Smith, N., 1998. Necessary conditions for a meandering-river avulsion. Geology 26, 435–438.
Smith, N., Cross, T., Dufficy, J., Clough, S., 1989. Anatomy of an avulsion. Sedimentology 36, 1–23.
Stanley, D., Warne, A., 1994. Worldwide initiation of Holocene marine deltas by deceleration of sea-level rise. Science 265 (5169), 228–231.
Stouthamer, E., Berendsen, H., 2007. Avulsion: the relative roles of autogenic and allogenic processes. Sedimentary Geology 198, 309–325.
Stouthamer, E., Berendsen, H.J.A., 2000. Factors controlling the Holocene avulsion history of the Rhine-Meuse delta (The Netherlands). Journal of Sedimentary Research 70, 1051–1064.
Struiksma, N., Olesen, K., Flokstra, C., De Vriend, H., 1985. Bed deformation in curved alluvial channels. Journal of Hydraulic Research 23, 57–79.
Syvitski, J., Saito, Y., 2007. Morphodynamics of deltas under the influence of humans. Global and Planetary Change 57, 261–282.
ten Brinke, W., Bolwidt, L., Snippen, F., van Hal, L., 2001. Sedimentbalans rijntakken 2000. Tech. Rep. RIZA2001.43, Rijkswaterstaat, Arnhem. . October.
Törnqvist, T., Weerts, H., Berendsen, H., 1994. Definition of two new members in the upper Kreftenheye and Twente formations (Quaternary, The Netherlands): a final solution to persistent confusion? Geologie en Mijnbouw 72, 251–264.
van Asselen, S., Stouthamer, E., van Asch, Th.W.J., 2009. Effects of peat compaction on delta evolution: a review on processes, responses, measuring and modeling. Earth Science Reviews 92, 35–51.
van de Ven, G., 1976. Aan de wieg van Rijkswaterstaat–wordingsgeschiedenis van het Pannerdens Kanaal (in Dutch). De Walburg Pers, Zutphen, The Netherlands.
van den Brink, P., 1998. In een opslag van het oog: de Hollandse rivierkartografie en waterstaatszorg in opkomst, 1725–1754 (in Dutch, river maps and waterway management in the province of Holland, 1725–1754). Utrecht University, Faculty of Geography.
van Rijn, L., 1993. Principles of Sediment Transport in Rivers, Estuaries and Coastal Seas. Aqua Publications, Oldemarkt.
Wang, Z., Fokkink, R., de Vries, M., Langerak, A., 1995. Stability of river bifurcations in 1d morphodynamic models. Journal of Hydraulic Research 33, 739–750.
Weerts, H., Cleveringa, P., Hendriks, J., de Bont, C., Maas, G., Meijer, T., Smit, B., 2005. The Last Avulsion of the Rhine (1421). International Conference for Fluvial Sedimentology 8, Delft, The Netherlands.
Zonneveld, I., 1960. De Brabantse Biesbosch, a Study of Soil and Vegetation of a Freshwater Tidal Delta. Vol. A,B,C. PUDOC Centrum voor Landbouwpublicaties, Wageningen, The Netherlands, published PhD-thesis.